ISBN: 978-3-95450-247-9 ISSN: 2673-5490 doi: 10.18429/JACoW-IPAC2024-MOPC73

DESIGN UPDATES TO THE EIC ELECTRON STORAGE RING LATTICE*

D. Marx†, E. Aschenauer, J.S. Berg, B. Bhandari, K. Hamdi, D. Holmes, J. Kewisch, Y. Li, E. Link, Y. Luo, C. Montag, S. Tepikian, D. Xu, Z. Zhang, Brookhaven National Laboratory, Upton, NY, USA
M.G. Signorelli, Cornell University, Ithaca, NY, USA
B.R. Gamage, D. Gaskell, Thomas Jefferson National Accelerator Facility, Newport News, VA, USA

Abstract

The Electron-Ion Collider (EIC) at Brookhaven National Laboratory will feature a 3.8-kilometer electron storage ring (ESR) that will circulate polarized beams with energies ranging from 5 to 18 GeV for collision with hadrons from a separate ring at luminosities up to $10^{34}\,\mathrm{cm^{-2}s^{-1}}$. This contribution focuses on several recent changes to the lattice design of the ESR. Super-bend dipole triplets are used in the arc cells to increase the damping decrement and horizontal emittance at 5 GeV. Their lengths have recently been optimized to balance these two requirements. The interaction region has been modified to accommodate the requirements of a Compton polarimeter. Major changes have been made to IR8, which is the location of a possible second interaction region and detector that may be installed in a future upgrade. A design for a non-colliding IR8 has been developed that simplifies the setup to reduce initial costs and complexity. The latest lattice design of the ESR is presented here, and the major design choices are discussed.

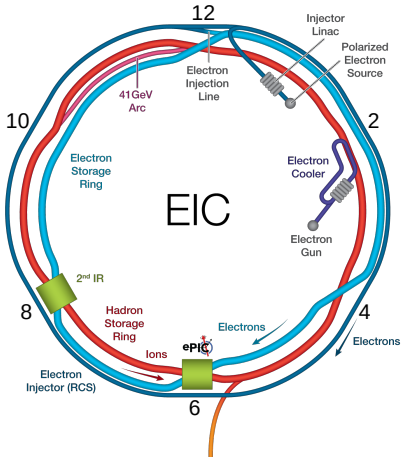

Figure 1: Schematic of EIC (not to scale), showing the rings that will be installed in the existing RHIC tunnel. The hadrons are injected from the AGS via the brown transfer line shown at the bottom of this image.

INTRODUCTION

The Electron-Ion Collider (EIC) [1, 2] will collide polarized electrons with polarized hadrons (protons up to heavy ions) for the purpose of investigating the structure and properties of nucleons. It will be built at Brookhaven National Laboratory in the 3.8-kilometer tunnel that currently houses the Relativistic Heavy Ion Collider (RHIC) [3–5]. Components from the two existing RHIC rings will be transformed into a new hadron storage ring, and two new electron rings will be built in this tunnel: a rapid cycling synchrotron (RCS) [6] for accelerating electrons to collision energies and an electron storage ring (ESR) [7, 8] for circulating electron beams for collisions. Figure 1 shows a schematic of the EIC. Collisions will occur at a range of center-of-mass energies between 29 GeV and 140 GeV, providing luminosities up to $10^{34}\,\mathrm{cm^{-2}s^{-1}}$. In order to achieve the desired range of center-of-mass energies, various combinations of electron and hadron beam energies will be collided. Three values for the electron beam energy are planned: 5, 10, and 18 GeV.

The ESR lattice consists of six arcs with insertion regions (IRs) in between, labeled according to the numbers on a clock face. The baseline design for the EIC includes a single interaction point, denoted IP6, where the beams will collide in the ePIC detector. A second interaction point and detector in the neighboring IR8 may be included in a future upgrade. Superconducting RF cavities will be installed in IR10, and the beam will be injected into the ring from the RCS in IR12. Overall, there will be three rings in the tunnel, as well as additional transfer lines and a bypass for low-energy hadron operation, resulting in very stringent space constraints. Achieving sufficient clearance between components while satisfying the geometric requirements of each individual beamline is a considerable challenge.

The ESR beamline will be located on the outside of the HSR for three arcs and on the inside for the other three arcs, with the paths crossing in IRs 4, 6, 8, and 12, as shown in Fig. 1. This arrangement helps to achieve synchronization between the electron and hadron bunches, since the path lengths must be almost equal [9]. A 200 µrad vertical tilt of the ESR centered on IPs 6 and 8 ensures sufficient vertical separation at IRs 4 and 12 for the ESR and HSR to cross without the need for vertical bending. In IR8 the two rings will be in the same vertical plane and therefore share a vacuum chamber, which requires the path lengths to be set appropriately to ensure that the bunches miss each other.

The design of the interaction region in IR6 is very challenging due to the many constraints imposed by the experimental program, as well as the tight space constraints in this region. Solenoid-based spin rotators located between the arc and the interaction region rotate the spin vector into or out of the longitudinal direction. The inner IR consists of dipoles whose bend angles are constrained by both the geometry and

* Work supported by Brookhaven Science Associates, LLC, under Contract No. DE-SC0012704 and by Jefferson Science Associates, LLC, under Contract No. DE-AC05-06OR23177 with the U.S. Department of Energy.
† dmarx@bnl.gov

ISBN: 978-3-95450-247-9 ISSN: 2673-5490 doi: 10.18429/JACoW-IPAC2024-MOPC73

the spin-polarization requirements, a number of matching quadrupoles, crab cavities, and various detectors.

This paper summarizes the recent changes to the ESR lattice, with specific focus on the super-bend dipoles in the arcs, the Compton polarimeter in the interaction region, and the IR8 crossover design.

SUPER-BEND DIPOLES

Two techniques are used to keep the horizontal emittance within an acceptable range over the wide energy range: varying the arc-cell phase advance and using super-bends in the arc cells [8]. The super-bends consist of two identical long dipoles (D1 and D3) and a shorter one in between (D2). At 10 and 18 GeV, all three dipoles produce a field in the same direction with the effect of a single dipole. At 5 GeV, however, the central dipole has reversed field, producing additional damping. This allows a larger beam-beam tune shift to be supported while increasing the horizontal equilibrium emittance. Both damping decrement and emittance scale with energy and bending radius, though the dependence is different: γ^3/ρ^2 for damping decrement [10] versus γ^2/ρ^3 for emittance in a pure FODO lattice [11]. This means that adjusting the lengths of the respective dipoles allows us to balance the damping decrement and emittance constraints. Consideration of the orbit excursion is also required to ensure a magnet with good field quality can be built despite the wide differences in orbit at different energies. The total length is maximized within the available longitudinal space in order to minimize the synchrotron radiation.

With these considerations in mind, the lengths of the super-bend dipoles were optimized. The magnetic length is now set to 2.726 m for the outer dipoles and 0.891 m for the central dipole. Figure 2 shows the trajectory through the super-bend dipole at different energies.

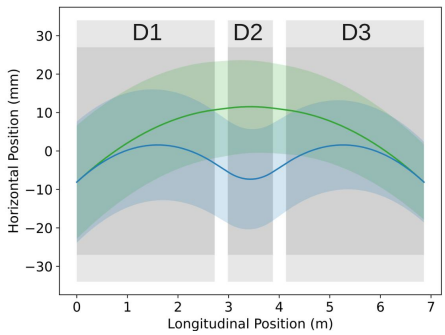

Figure 2: Trajectory through a super-bend triplet in the arcs. The trajectory at 10 and 18 GeV is shown in green, and the trajectory at 5 GeV is shown in blue. The colored shaded areas are the 15σ beam envelopes.

INTERACTION REGION

Electron and hadron beams will collide at IP6 with a crossing angle of 25 mrad. Due to the nature of electron-hadron collisions, the interaction region is very asymmetrical. There are tight geometric requirements arising from the constraints in the tunnel, as well as specific bend angles dictated by spin requirements. Synchrotron radiation is a major concern, especially surrounding important detector components.

A Compton polarimeter is located on the upstream side of the IP for the electrons. A laser is shone at the electron beam, dipoles bend the electrons away from the scattered photons, and electrons and photons are then detected by respective detectors. There are many constraints on the layout and optics arising from this setup. In particular, there are requirements on the beam size at the laser IP, the bend angles in order to limit synchrotron radiation at the photon detector, and the R_{16} at the electron detector to detect the energy difference in the scattered electrons. This section has been redesigned to satisfy these requirements adequately for polarimetry measurements. Its geometric layout is shown in Fig. 3.

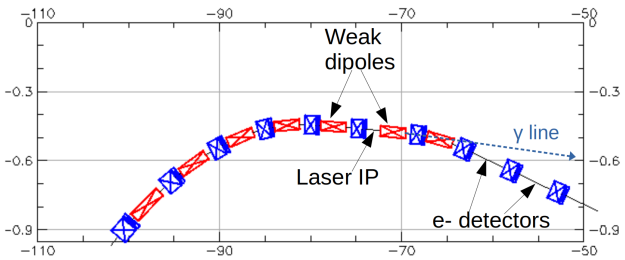

Figure 3: Floor plan of the IR6 section containing the Compton polarimeter. Axes units are meters, and the electron beam travels from left to right. Dipoles are shown in red and quadrupoles in blue. All dipoles are 2.726 m long, but the two labeled weak dipoles only have a bending angle of 1.5 mrad, as opposed to 12–13 mrad for the others.

IR8

IR8 is designated as the location of a second IP and detector as part of a possible future upgrade. Initially, however, a simple, economical crossover will be installed. This will be similar to the crossovers in IRs 12 and 4, although the ESR and HSR will be in the same plane in IR8, so the path lengths must be set to ensure that bunches miss each other at the crossover while colliding at IP6. This is in fact the same condition required when operating with two IPs [9]. In addition, the total path length for the ring should be set to match the revolution time of the hadrons. Although the design for a second interaction region is still at the conceptual stage, care has been taken to set the path lengths so that this could be installed locally without the need for substantial modifications in the rest of the ring. A design for a non-colliding IR8 has been proposed that uses 32 dipoles, including four bending in the reverse direction, to meet the path-length conditions. The geometric layout is shown in Fig. 4.

GEOMETRY

Overall, arranging all the beamlines required for the EIC in the RHIC tunnel represents a significant challenge. Beam-

ISBN: 978-3-95450-247-9 ISSN: 2673-5490 doi: 10.18429/JACoW-IPAC2024-MOPC73

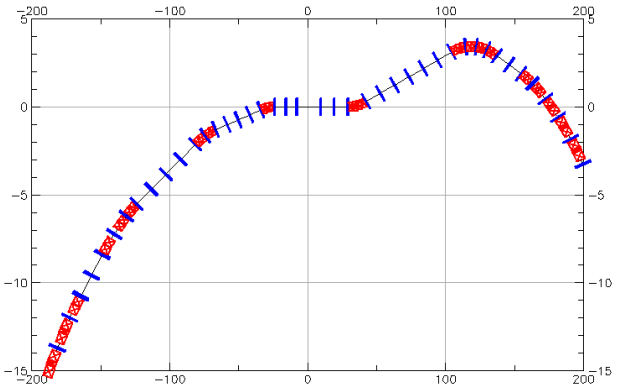

Figure 4: Floor plan of IR8. Axes units are meters, and the electron beam travels from left to right. Dipoles are shown in red and quadrupoles in blue. All dipoles are 2.726 m long.

line elements must be carefully placed to avoid interferences with other beamlines and the tunnel walls. In many cases, the clearance between elements is only a few centimeters. There are many additional constraints on the bending angles in the ESR arising from polarization requirements and the need to reduce synchrotron radiation, both globally and locally. Much work has been done to eliminate geometric interferences while satisfying all the constraints on bending angles. Figure 5 shows a representation of the geometric layout of the whole ring.

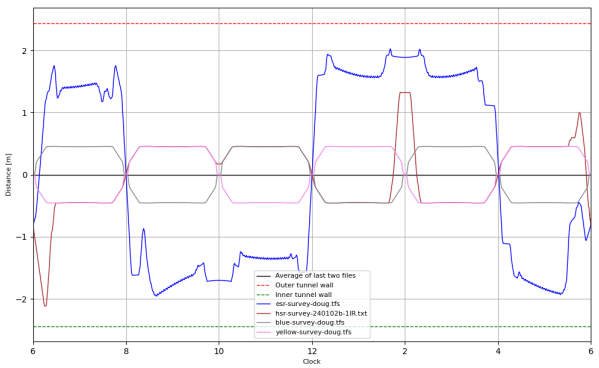

Figure 5: Layout of rings in the tunnel. The horizontal axis shows the angle along the ring in terms of the numbers on a clock face. The vertical axis shows radial distance from the tunnel center, with the green and red dotted lines indicating the inner and outer tunnel walls. The ESR beamline (blue) is shown alongside the HSR beamline (brown) and the two existing RHIC rings (gray and pink lines). Parts of the RHIC rings that are not being used in the HSR will be removed.

OPTICS

Figure 6 shows the matched optics for the 18 GeV lattice with one IP while Table 1 shows the main parameters for this lattice. The optics are periodic in the arcs, with the phase advance set to 90° at 18 GeV and 60° at 5 and 10 GeV. There is also some periodicity in some of the IRs, primarily to reduce the number of required power supplies. The phase advances

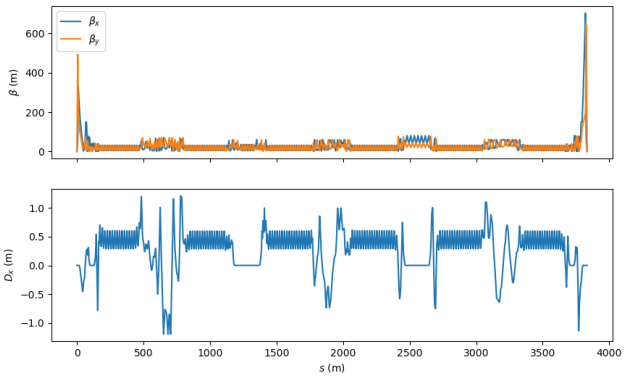

Figure 6: β functions and dispersion for matched ring with 1 IP.

Table 1: ESR Lattice Parameters at 18 GeV with 1 IP

Parameter	Value
Arc cell phase adv.	90°
Hor. emit. (nm)	30
Energy spread	0.096%
β_x^*/β_y^* (m)	0.59 / 0.057
Tunes, Q_x/Q_y	48.08 / 44.14
Nat. chrom., ξ_x/ξ_y	-88 / -90

between arcs will be used as variables in the optimization of the dynamic aperture [12, 13], so these are expected to change from the current linear optics match shown here. The global tune is fixed and was chosen to be suitable for beam-beam as well as polarization performance [14].

CONCLUSION

Much work has been performed recently to resolve outstanding issues with the ESR lattice design. The lengths of the super-bend dipoles in the arcs have been optimized. The upstream side of the interaction region has been redesigned to accommodate a Compton polarimeter. A design for an initial non-colliding IR8 has been developed. Many other modifications have also been made to avoid interferences in the tunnel. Magnet lengths have been chosen with regard to reducing the number of new magnets that will have to be designed and built, and reusing existing magnets from the APS where possible [15].

There is an ongoing study into optimizing the design of the spin rotators to meet technical constraints while satisfying the challenging optics-matching requirements. Local coupling correction in the interaction region at IP6 needs to be incorporated into the lattice. Furthermore, locations of collimators, correctors, and diagnostics need to be settled on.

REFERENCES

[1] J. Beebe-Wang *et al.*, "Electron-Ion Collider: Conceptual Design Report", Brookhaven National Laboratory, Jefferson Lab, 2021. `www.bnl.gov/EC/files/EIC_CDR_Final.pdf`

ISBN: 978-3-95450-247-9 ISSN: 2673-5490 doi: 10.18429/JACoW-IPAC2024-MOPC73

[2] C. Montag *et al.*, "The EIC accelerator – design highlights and project status", presented at IPAC'24, Nashville, TN, USA, May 2024, paper MOPC67, this conference.

[3] C. Montag, "RHIC status and plans", *AIP Conference Proceedings*, vol. 2160, no. 1, p. 040 006, 2019. doi:10.1063/1.5127686

[4] "RHIC Configuration Manual", Brookhaven National Laboratory, 2006. www.bnl.gov/cad/accelerator/docs/pdf/RHICConfManual.pdf

[5] K. Hübner *et al.*, "The largest accelerators and colliders of their time", in *Particle Physics Reference Library : Volume 3: Accelerators and Colliders*, 2020. doi:10.1007/978-3-030-34245-6_10

[6] H. Lovelace, C. Montag, F. Lin, and V. Ranjbar, "An update on EIC rapid cycling synchrotron optics", presented at IPAC'24, Nashville, TN, USA, May 2024, paper MOPG02, this conference.

[7] D. Marx *et al.*, "Lattice design of the EIC electron storage ring for energies down to 5 GeV", in *Proc. IPAC'23*, Venice, Italy, 2023, pp. 104–107. doi:10.18429/JACoW-IPAC2023-MOPA037

[8] D. Marx *et al.*, "Designing the eic electron storage ring lattice for a wide energy range", *Journal of Physics: Conference Series*, vol. 2420, no. 1, p. 012 010, 2023. doi:10.1088/1742-6596/2420/1/012010

[9] J. Berg *et al.*, "Synchronizing the timing of the electron and Hadron storage rings in the Electron-Ion Collider", in *Proc. IPAC'23*, Venice, Italy, 2023, pp. 906–908. doi:10.18429/JACoW-IPAC2023-MOPL157

[10] H. Wiedemann, *Particle accelerator physics*. Springer Berlin Heidelberg, 2015.

[11] S. Peggs and T. Satogata, *Introduction to Accelerator Dynamics*. Cambridge University Press, 2017.

[12] Y. Cai *et al.*, "Optimization of chromatic optics in the electron storage ring of the electron-ion collider", *Phys. Rev. Accel. Beams*, vol. 25, no. 7, p. 071 001, 2022. doi:10.1103/PhysRevAccelBeams.25.071001

[13] Y. Nosochkov *et al.*, "Dynamic aperture of the EIC electron storage ring", presented at IPAC'24, Nashville, TN, USA, May 2024, paper MOPC82, this conference.

[14] Y. Luo *et al.*, "Optimizing the design tunes of the electron storage ring of the Electron-Ion Collider", in *Proc. IPAC'23*, Venice, Italy, 2023, pp. 128–131. doi:10.18429/JACoW-IPAC2023-MOPA047

[15] C. Montag *et al.*, "Recycling magnets for the EIC electron storage ring", presented at IPAC'24, Nashville, TN, USA, May 2024, paper MOPC64, this conference.